

REPORT DOCUMENTATION PAGE

Form Approved
OMB No. 0704-0188

The public reporting burden for this collection of information is estimated to average 1 hour per response, including the time for reviewing instructions, searching existing data sources, gathering and maintaining the data needed, and completing and reviewing the collection of information. Send comments regarding this burden estimate or any other aspect of this collection of information, including suggestions for reducing the burden, to Department of Defense, Washington Headquarters Services, Directorate for Information Operations and Reports (0704-0188), 1215 Jefferson Davis Highway, Suite 1204, Arlington, VA 22202-4302. Respondents should be aware that notwithstanding any other provision of law, no person shall be subject to any penalty for failing to comply with a collection of information if it does not display a currently valid OMB control number.

PLEASE DO NOT RETURN YOUR FORM TO THE ABOVE ADDRESS.

1. REPORT DATE (DD-MM-YYYY) 04/17/2007			2. REPORT TYPE Final Report		3. DATES COVERED (From - To) 6/15/06 - 12/30/2006	
4. TITLE AND SUBTITLE Meso-scale self-assembly pilot study					5a. CONTRACT NUMBER N00014-06-1-0578	
					5b. GRANT NUMBER N00014-06-1-0578	
					5c. PROGRAM ELEMENT NUMBER	
6. AUTHOR(S) Babak AmirParviz					5d. PROJECT NUMBER	
					5e. TASK NUMBER	
					5f. WORK UNIT NUMBER	
7. PERFORMING ORGANIZATION NAME(S) AND ADDRESS(ES) University of Washington Dept. of Electrical Engineering, Box 352500 Seattle, WA 98195-2500					8. PERFORMING ORGANIZATION REPORT NUMBER	
9. SPONSORING/MONITORING AGENCY NAME(S) AND ADDRESS(ES) Office of Naval Research 1107 NE 45th Street Suite 350 Seattle, WA 98105-4631					10. SPONSOR/MONITOR'S ACRONYM(S)	
					11. SPONSOR/MONITOR'S REPORT NUMBER(S)	
12. DISTRIBUTION/AVAILABILITY STATEMENT Approved for Public Release						
13. SUPPLEMENTARY NOTES						
14. ABSTRACT The project investigates the formation of micro-scale structures using capillary force-driven self-assembly. Two main activities were undertaken during the course of the project: determination of the proper self-assembly environment and scaling of the metal contacts, and development of microfabrication processes that can generate micron-scale single crystal silicon parts that can participate in a self-assembly process. The effect of the alloy composition, chemical composition of the self-assembly environment, and contact metallization were extensively studied and an optimum condition for scaling the metal contacts was determined. Microfabrication processes on SOI wafers were developed to form parts that can participate in 2D and 3D self-assembly processes.						
15. SUBJECT TERMS						
16. SECURITY CLASSIFICATION OF:			17. LIMITATION OF ABSTRACT SAR	18. NUMBER OF PAGES 8	19a. NAME OF RESPONSIBLE PERSON Babak AmirParviz	
a. REPORT U	b. ABSTRACT U	c. THIS PAGE U			19b. TELEPHONE NUMBER (Include area code) 206-616-4038	

Final Report

Summary

The goal was to make progress toward self-assembling three-dimensional circuits using a molten alloy, exploring the feasibility of future programs for DARPA in both three-dimensional integrated circuits and heterogeneous integration. The progress to date includes:

- The determination of a fluid environment in which an alloy of choice does not corrode excessively, and demonstration of self-assembly using simple, single-contact parts.
- Microfabrication procedure for constructing parts with the necessary topography to realize 3D self-assembly.

Contents

Summary	1
Contents.....	1
Details.....	1
Introduction	1
Alloy and Fluid Environment Experiments.....	2
Methods	2
Results	3
1-D Self-assembly	4
Methods	4
Results	5
3D Self-Assembly Part Fabrication.....	7
References	8

Details

Introduction

Advances in electronics and microelectromechanical systems (MEMS) continue to enable smaller, faster, cheaper, and more integrated systems. Despite this progress, efforts in the area of integration have faced significant challenges in constructing 3D structures, and building heterogeneous integrated systems made of parts from incompatible microfabrication processes. Although robotic “pick-and-place” techniques are currently used to integrate devices from many types of processes, the ability to efficiently handle individual parts diminishes as the size scale of the components

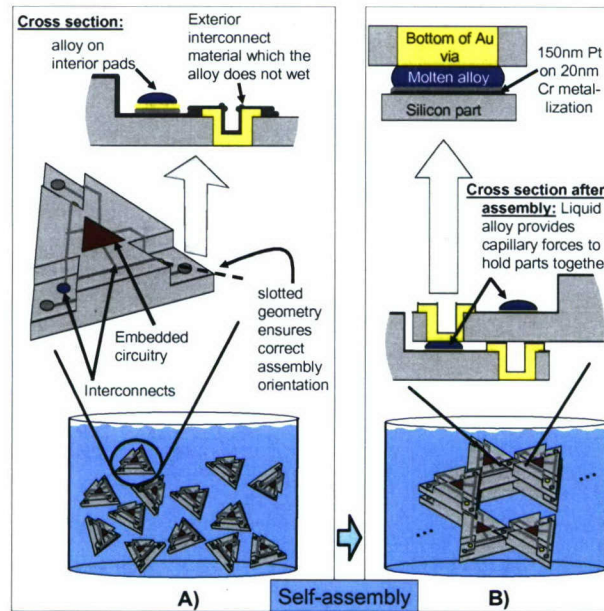


Fig. 1: Schematic showing 3D, triangular parts (A) which can assemble into a 3D circuit when submersed and agitated in a fluid (B).

decreases below about $300\ \mu\text{m}$ [1]. Self-assembly, or the spontaneous organization of parts into larger structures via energy minimization, is an attractive solution to overcome current integration limitations.

One way to create electrical and mechanical connections with self-assembly is to use capillary forces from a molten alloy. Many research groups have employed molten alloys at small scales for self-assembly combined with other driving mechanisms such as gravity [2] or magnetic fields [3]. Those using capillary forces exclusively [4] do so at size scales of $200\ \mu\text{m}$ and larger. At least one reason is that molten alloys typically require an acid flux to clean oxides off alloy surfaces, and the process of alloy oxidation and oxide reduction continually removes alloy material. This process ultimately limits the scale to which molten alloy structures can be miniaturized, and is therefore of great importance to whether self-assembly can overcome future integration challenges.

Fig. 1 shows a model system for the investigation of 3D, small scale integration by self-assembly. The triangular parts in Fig. 1A) feature a slotted geometry for complimentary shape recognition which insures correct orientation upon assembly, and a solder alloy deposited on the interior region of the slot. Also, electrical vias near the exterior of the slot provide alloy-wettable binding sites on the underside, and an interconnect material which is not wettable by the alloy prevents incorrect alloy binding. Fig. 1B) shows 3D self-assembled structures, and a cross sectional detail of the 3D electrical interconnects.

Alloy and Fluid Environment Experiments

Methods

To realize assembly of the parts depicted in Fig. 1, an appropriate alloy and self-assembly fluid system must be determined which will allow the alloy to wet and bind to the desired surfaces. Nearly all demonstrations of integration by molten-alloy based,

capillary-force driven self-assembly to date use a eutectic Bi-Pb-In-Sn-Cd alloy melting at 47°C, and water or ethylene glycol (EG) as the self-assembly fluid. However, the alloy's five component composition makes it difficult to study or alter its corrosion-related properties. Eutectic 58Bi-Sn solder melting at 138 °C was attractive for its lead-free status and low oxidation rate compared to many other solders [5], so we chose this alloy to study. We tested this alloy in nine fluids, including EG, EG with sodium nitrite (NaNO₂) or sodium benzoate (SB) as anti corrosion agents [6], glycerol, hexadecane, 1-octanol, and three ionic liquids based on Choline Chloride (ChCl), one of which has been used for plating Zn-Sn compounds [7].

We fabricated test templates by evaporating a metal multilayer of 20 nm Cr, 100-150 nm Ni or Pt, and 100 nm Au, and patterning the multilayer into features using photolithography and lift-off. Ongoing research in our group concerns the fabrication of silicon parts for self-assembly into three-dimensional electrical networks. A first generation design of these parts included 20 μm diameter alloy regions, so the present study concerns similarly-sized features. We used the dip coating procedure in [2] to deposit the alloy on the patterned metal features, which involves retracting a template from a molten alloy bath through a layer of EG, where the low contact angle of EG on silicon and/or SiO₂ prevented solder from settling on the rest of the substrate.

Energy-dispersive x-ray spectroscopy (EDX) before and after exposure to a liquid at 150°C revealed the composition change of the alloy "bumps," and indicated whether significant corrosion occurred. Once we found a suitable liquid that did not significantly change the alloy composition with time, we conducted similar tests with different concentrations of HCl in that fluid to determine the rate at which the oxidation/reduction reactions occur on alloy features at this scale.

Results

The first templates contained a Cr/Ni/Au metal layer, with 100 nm of Ni, and Fig. 3 shows how the composition of the 58Bi-Sn alloy on these templates varied with time in EG at 150°C. The EDX plots in Fig. 3 show a significant Si signal, indicating that the electron beam used to generate the EDX data had enough energy to penetrate a significant portion of the 3–4 μm high alloy bumps. Thus, the EDX data may be interpreted as an average alloy bump composition, although the local composition varied significantly. The Bi concentration initially increased, while the relative amount of Sn decreased, suggesting EG initially attacks Sn. After approximately 14 minutes, the Sn and Ni percentages sharply increased, accompanied by a decrease in Bi which eventually approached zero, indicating the Bi was being attacked as well. The final atomic ratio of Ni:Sn was approximately 3:4, indicating a Ni₃Sn₄ IMC, which is the primary Ni-Sn IMC at these temperatures [8].

The Bi composition during exposure to the nine different candidate fluids is shown in Fig. 4. Hexadecane, glycerol, and 1-octanol did not change the alloy composition significantly, and only the latter two were able to dissolve the alloy's oxide reduction product. Operating at a higher temperature of 180°C, we repeatedly saw small bubbles originating at alloy surfaces in 1-octanol, but not in glycerol. The bubbles may have resulted from 1-octanol being close to its boiling point (197°C). Thus, glycerol was the fluid of choice, and Fig. 2 shows how the alloy fared at different HCl concentrations in glycerol at 180°C. Fig. 2 indicates that a concentration of no more than 0.1 mM should allow the alloy to function properly for the times shown.

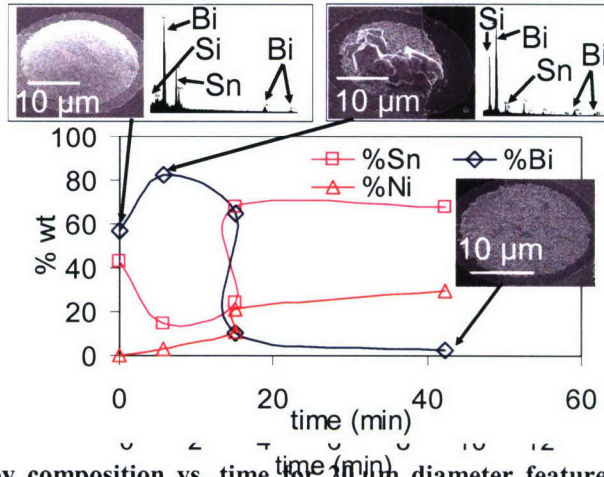


Fig. 3: 58Bi-Sn Alloy composition vs. time for 20 μm diameter features in ethylene glycol at 150°C, as determined by energy-dispersive x-ray spectroscopy (EDX).

Fig. 2: Bi composition of alloy (30 μm diameter features) as a function of time in glycerol at 180°C with various HCl concent

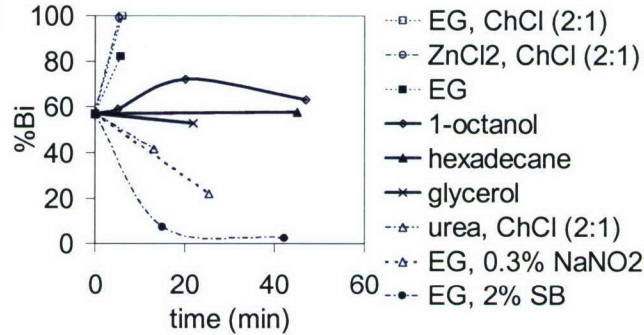


Fig. 4: Bi composition of alloy (30 μm diameter features) as a function of time in various solutions at 150°C, determined by EDX.

The templates in Fig. 2 and those in all subsequent tests had a 150 nm Pt layer instead of Ni, because we found the alloy to easily detach from the template when the Ni-Sn IMC consumed the entire Ni layer. Pt is a much better diffusion barrier to IMC growth [9].

1-D Self-assembly

Methods

Once a suitable fluid environment was determined, we fabricated parts to test the assembly process using capillary forces as shown in Fig. 5. Starting with a silicon-on-oxide wafer having a 10, 20, or 50 μm thick device layer, the same lift-off procedure used for the templates served to pattern metal contacts on the parts. Next, a deep-reactive ion etch down to the buried oxide layer defined part sidewalls, and finally, a buffered-oxide etch (BOE) released the parts into a filter for transfer into the carrier fluid, de-ionized (DI) water.

For a self-assembly experiment, we transferred parts into a vial and added a 3:7 $\text{H}_2\text{O}_2:\text{H}_2\text{SO}_4$ “piranha” solution for one minute to insure clean, metal contacts. We then rinsed the parts with DI water, suspended them in ethanol, added 4 ml of glycerol, heated the mixture to 100°C to evaporate any remaining ethanol, cooled the vial to room temperature, and added a template as shown in Fig. 5. We placed the vial in a 215°C

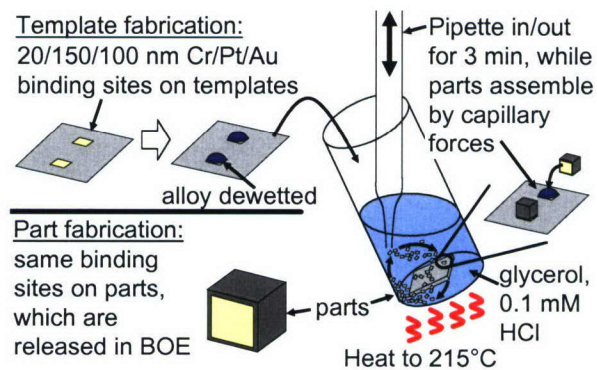


Fig. 5: Schematic diagrams showing how templates and parts are fabricated for self-assembly experiments, and how parts assemble on binding sites.

glycerol bath for 30 seconds, allowing the temperature to rise above the alloy melting point, and commenced the agitation depicted in Fig. 5. The aspiration and discharge of approximately 1 ml of fluid (and parts) every 1-10 seconds using a Pasteur pipette stirred up parts at the base of the container and allowed them to gently fall across the template. Self-assembly happened whenever one of the parts contacted a functional solder bump, after which capillary forces held the part in place.

Results

To ultimately test the alloy's capillary functionality at small scales, Fig. 6 shows the result of assembling 100 μm diameter parts following the procedure outlined in the methods section. The yield was about 97% for roughly 2000 parts assembled in 2.5 minutes. Moving down in scale, Fig. 7 shows the assembly of 40 μm square parts at 84% yield (or approximately 8400 assembled in 2.5 minutes), and 20 μm diameter parts at 15% yield. In each of these tests, the total part to container fluid volume was held constant, at 1%. We dropped the rate of agitation from 1 Hz to 0.1 Hz as the part size decreased, because the settling time was much less due to lower part mass.

To investigate why the yield drops so drastically, Fig. 8 shows identically-sized 100 μm diameter parts with different contact pad diameters (as shown at the top of Fig. 8). Each type of part was self-assembled under similar conditions on templates with the alloy pattern diameters shown in the legend of the figure. The results were remarkably similar for each part, regardless of what type of template on which they were assembled. These results could be explained by a need to have large part contacts, but the 40 μm parts in Fig. 7 would not fit with this explanation.

Despite the partial understanding presented here, we conclude that self-assembly using a higher melting point alloy works well with parts having contacts down to 40 μm in size. These results enable our continued work on self-assembly with parts incorporating the ability to assemble in three dimensions.

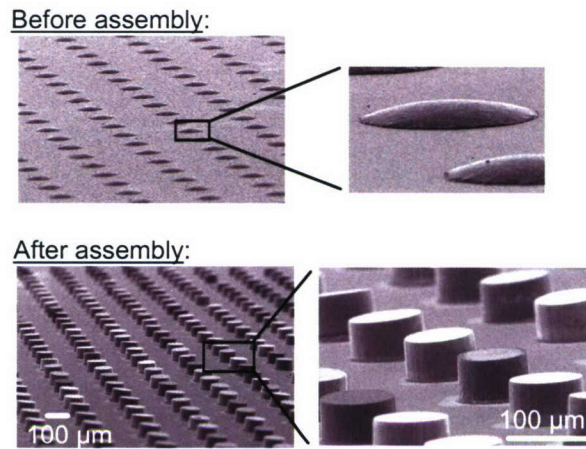


Fig. 6: Self-assembly with 100 μm diameter, 50 μm tall parts exhibiting 97% yield.

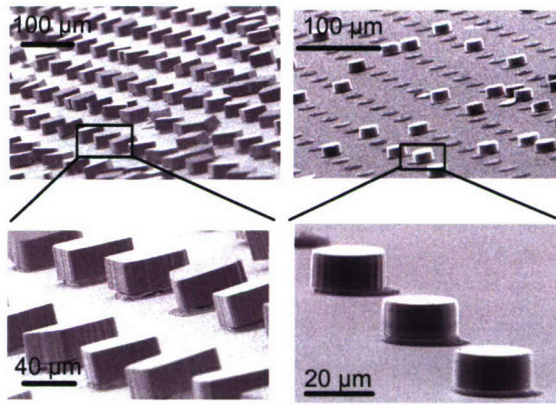


Fig. 7: Self-assembly with 40 μm square, 20 μm tall parts (85% yield), and with 20 μm diameter, 10 μm tall parts (15% yield).

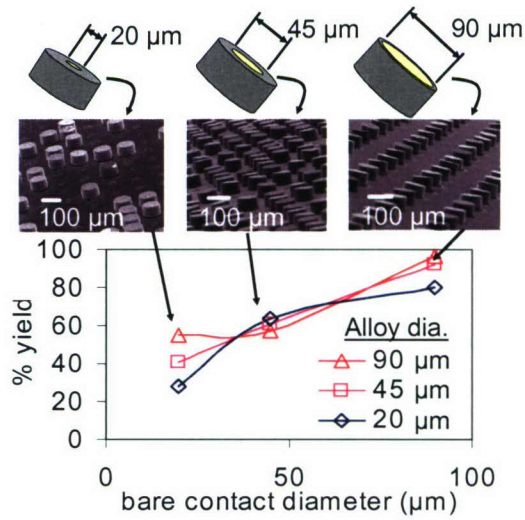


Fig. 8: Self-assembly yield vs. contact diameters for different alloy diameters on templates.

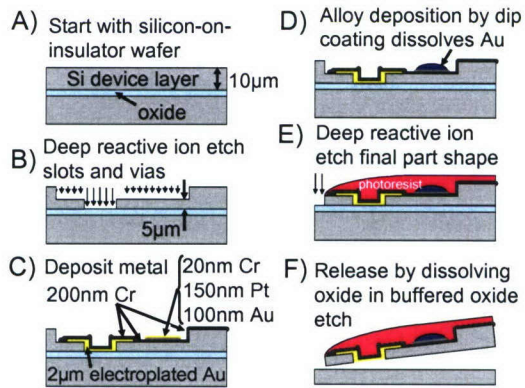


Fig. 9: Fabrication process for parts shown in Fig. 1.

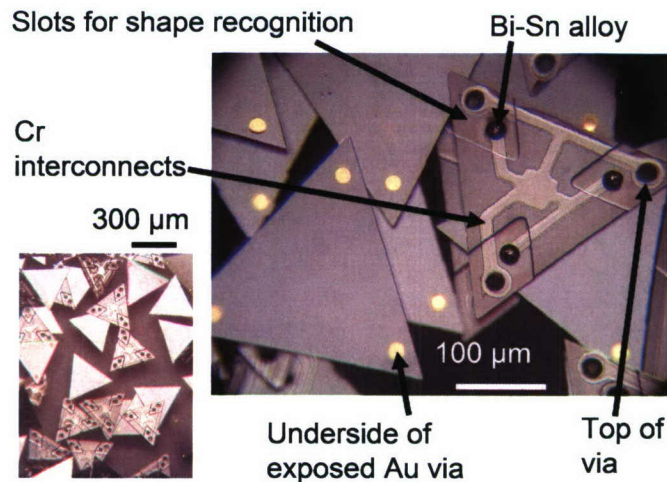


Fig. 10: Released and fabricated parts ready for the assembly shown in Fig. 1

3D Self-Assembly Part Fabrication

With the determination of an appropriate alloy and self-assembly fluid system, we fabricated the parts depicted in Fig. 1 using the process flow outlined in Fig. 9. We started with a silicon-on-insulator (SOI) wafer with a 10 μm device layer (Fig. 9A). The slotted geometry was defined with a deep reactive ion etch (DRIE), and vias were defined with another 5 μm DRIE step (Fig. 9B). Fig. 9C) shows the vias filled with 2 μm of electroplated Au, an evaporated Cr interconnect layer (200 nm), and the alloy metallization layer (20 nm Cr, 150 nm Pt, 100 nm Au). Next, in Fig. 9D) the alloy, a lead-free eutectic Bi-Sn solder melting at 138 $^{\circ}\text{C}$, was dewetted onto the metallization features by first evaporating 100 nm of Au, and then dipping the Au-coated wafer substrate through a 160 $^{\circ}\text{C}$ ethylene glycol/molten alloy interface. The evaporated Au insured that the alloy wetted the entire substrate, and most of the Au quickly dissolved allowing the alloy to react with the Pt layer. When the substrate was retracted, the alloy dewets from all Si and Cr areas, leaving the alloy only at the prescribed locations. Without the Au layer, the alloy rarely wetted the Pt patterns which were located at the

bottom of the 5 μm recesses. In Fig. 9E) the final part shape is defined with DRIE, and in Fig. 9F) the photoresist is left on while the oxide is dissolved in buffered oxide etch (BOE) for 27 hr. Fig. 10 shows the released parts after the remaining photoresist has been stripped, and the 20 μm diameter alloy regions are visible.

References

- [1] C. J. Morris, S. A. Stauth, and B. A. Parviz, "Self-assembly for micro and nano scale packaging: Steps toward self-packaging," *IEEE Trans. Adv. Packag.*, vol. 28, no. 4, pp. 600-611, 2005.
- [2] S. Stauth and B. A. Parviz, "Self-assembled silicon networks on plastic," in Proc. 13th Int. Conf. on Solid State Sens. Actuators (Transducers '05), Seoul, Korea, pp. 964-967, 2005.
- [3] H. Ye, Z. Gu, T. Yu, and D. H. Gracias, "Integrating nanowires with substrates using directed assembly and nanoscale soldering," *IEEE Transactions on Nanotechnology*, vol. 5, no. 1, pp. 62 - 6, 2006.
- [4] J. Chung, W. Zheng, T. J. Hatch, and H. O. Jacobs, "Programmable reconfigurable self-assembly: Parallel heterogeneous integration of chip-scale components on planar and nonplanar surfaces," *J. Microelectromech. Sys.*, vol. 15, no. 3, pp. 457-464, 2006.
- [5] G. D. Giacomo, K. L. Granato, H. Shaukatullah, F. Casullo, and R. Guarnieri, "Oxidation kinetics of Bi-Sn eutectic films and thermal contact resistance," in Proc. International Symposium on Microelectronics, Minneapolis, MN, USA, pp. 587 - 93, 1987.
- [6] I. L. v. Rozenfeld, *Corrosion inhibitors (translation of inhibitory korrozii)*: McGraw-Hill, 1981.
- [7] A. P. Abbott, G. Capper, D. L. Davies, R. K. Rasheed, and V. Tambyrajah, "Novel ambient temperature ionic liquids for zinc and zinc alloy electrodeposition," *Trans. Inst. Met. Finish.*, vol. 79, pp. 204-206, 2001.
- [8] G. Ghosh, "Interfacial microstructure and the kinetics of interfacial reaction in diffusion couples between Sn-Pb solder and Cu/Ni/Pd metallization," *Acta Materialia*, vol. 48, no. 14, pp. 3719-3738, 2000.
- [9] J. F. Kuhmann, C. H. Chiang, P. Harde, F. Reier, W. Oesterle, I. Urban, and A. Klein, "Pt thin-film metallization for FC-bonding using SnPb60/40 solder bump metallurgy," *Mater. Sci. & Eng. A*, vol. 242, no. 1-2, pp. 22 - 5, 1998.